Hypoxia Epigenetically Confers Astrocytic Differentiation Potential on Human Pluripotent Cell-Derived Neural Precursor Cells

安井, 徹郎

https://doi.org/10.15017/1928622

出版情報：九州大学, 2017, 博士（医学）, 課程博士
バージョン：

Stem Cell Reports
Article

OPEN ACCESS

Hypoxia Epigenetically Confers Astrocytic Differentiation Potential on Human Pluripotent Cell-Derived Neural Precursor Cells

Tetsuro Yasui,[1,2] Naohiro Uezono,[1] Hideyuki Nakashima,[1] Hirofumi Noguchi,[1] Taito Matsuda,[1] Tomoko Noda-Andoh,[3] Hideyuki Okano,[3] and Kinichi Nakashima[1,4,*]

[1]Department of Stem Cell Biology and Medicine
[2]Department of Otorhinolaryngology
Graduate School of Medical Sciences, Kyushu University, 3-1-1 Maidashi, Higashi-ku, Fukuoka, Fukuoka 812-8582, Japan
[3]Department of Physiology, School of Medicine, Keio University, 35 Shinanomachi, Shinjuku-ku, Tokyo 160-8582, Japan
[4]Laboratory of Molecular Neuroscience, Graduate School of Biological Sciences, Nara Institute of Science and Technology, Ikoma, Nara 630-0192, Japan
*Correspondence: kin1@scb.med.kyushu-u.ac.jp
http://dx.doi.org/10.1016/j.stemcr.2017.05.001

SUMMARY

Human neural precursor cells (hNPCs) derived from pluripotent stem cells display a high propensity for neuronal differentiation, but they require long-term culturing to differentiate efficiently into astrocytes. The mechanisms underlying this biased fate specification of hNPCs remain elusive. Here, we show that hypoxia confers astrocytic differentiation potential on hNPCs through epigenetic gene regulation, and that this was achieved by cooperation between hypoxia-inducible factor 1α and Notch signaling, accompanied by a reduction of DNA methylation level in the promoter region of a typical astrocyte-specific gene, *Glial fibrillary acidic protein*. Furthermore, we found that this hypoxic culture condition could be applied to rapid generation of astrocytes from Rett syndrome patient-derived hNPCs, and that these astrocytes impaired neuronal development. Thus, our findings shed further light on the molecular mechanisms regulating hNPC differentiation and provide attractive tools for the development of therapeutic strategies for treating astrocyte-mediated neurological disorders.

INTRODUCTION

The mammalian CNS is composed mainly of three neural cell types, neurons, astrocytes, and oligodendrocytes, all of which are generated from common multipotent neural precursor cells (NPCs) (Namihira and Nakashima, 2013; Svendsen et al., 1998). With recent advances in stem cell culture techniques, NPCs derived from human pluripotent stem cells (hPSCs), and embryonic and induced pluripotent stem cells (hESCs and hiPSCs), have been shown to recapitulate neural development to some extent in vitro (Takahashi et al., 2007; Thomson et al., 1998; Yu et al., 2007) and to serve as a model for various neurological disorders (Israel et al., 2012; Marchetto et al., 2011; Park et al., 2008; Sanchez-Danes et al., 2012). However, although human NPCs (hNPCs) derived from hPSCs differentiate efficiently into neurons, an extremely low fraction of them generate astrocytes over a period of 4 weeks after the induction of differentiation (Hu et al., 2010). Recent studies have shown that hNPCs require prolonged culture (typically around 100–200 days) under sphere-forming conditions to efficiently differentiate into astrocytes (Edri et al., 2015; Kondo et al., 2013; Krencik et al., 2011; Williams et al., 2014), thus retarding human astrocyte functional research that is relevant to neurological diseases.

Constituting about 40% of all cells in the brain, astrocytes have long been classified as mere passive supporting cells that, for example, promote survival and functional synaptic formation of neurons; however, astrocytes are also essential for the phagocytic elimination of synapses, which refines neuronal circuit development (Allen and Barres, 2009). Because these roles of astrocytes are very important for brain function, astrocytes are indispensable components in CNS integrity (Allen et al., 2012; Christopherson et al., 2005; Hamilton and Attwell, 2010; Haydon and Nedergaard, 2015; Kucukdereli et al., 2011; Molofsky et al., 2012; Ullian et al., 2001; Zhang et al., 2016). Therefore, astrocyte dysfunction is thought to be implicated in various neurological disorders including Rett syndrome (RTT), which is caused by methyl-CpG binding protein 2 (*MECP2*) mutations (Amir et al., 1999; Bienvenu and Chelly, 2006; Tsujimura et al., 2015). Mutant (MT) MECP2-expressing astrocytes derived from RTT-hiPSCs have recently been reported to have adverse effects on neuronal maturation compared with their isogenic wild-type (WT) MECP2-expressing astrocytes (Williams et al., 2014). However, little progress in human astrocyte functional analysis has been made because, as noted above, differentiation of hPSC-derived hNPCs into astrocytes is a time-consuming process.

The interleukin-6 family of cytokines, including leukemia inhibitory factor (LIF), are well known to efficiently induce astrocytic differentiation of late-gestational (lg) NPCs by activating the janus kinase (JAK)-signal transducer and activator of transcription (STAT) signaling

pathway (Bonni et al., 1997; Nakashima et al., 1999; Weible and Chan-Ling, 2007). However, these cytokines are incapable of inducing astrocytic differentiation of mid-gestational (mg)NPCs because astrocytic genes, such as *Glial fibrillary acidic protein* (*Gfap*), are silenced by DNA methylation (Fan et al., 2005; Takizawa et al., 2001). Thus, mgNPCs have a strong tendency to differentiate into neurons rather than astrocytes. mgNPCs prepared from embryonic day 11 (E11) mouse telencephalon can be induced with moderate efficiency to differentiate into astrocytes after culturing for 4 days (nominally corresponding to E15), while astrocytic differentiation is effectively induced in lgNPCs prepared directly from E15 mouse telencephalon. We have previously shown that this weaker acquisition of astrocytic differentiation potential by mgNPCs cultured in dishes is due to the high oxygen level compared with that in vivo (Mutoh et al., 2012). The atmosphere contains 21% O_2 (160 mm Hg), whereas interstitial oxygen concentration ranges from 1% to 5% (7–40 mm Hg) in mammalian tissues including the embryonic brain (Mohyeldin et al., 2010; Simon and Keith, 2008). Thus, 21% O_2 (atmospheric) is actually physiologically abnormal in vivo; however, because cell cultures are generally conducted in 21% O_2, and it is common to define atmospheric O_2 concentration as normoxia, we refer to 21% O_2 as normoxia in this study. Notably, when we cultured E11 mgNPCs for 4 days under hypoxia (2% O_2), the cells differentiated efficiently into astrocytes, to a level comparable with that of E15 lgNPCs. We also revealed that demethylation of *Gfap* in mgNPCs is enhanced in hypoxic culture compared with that in normoxia (21%) (Mutoh et al., 2012).

Given these findings, we hypothesized that the inefficient astrocytic differentiation of hPSC-derived hNPCs is due to a retarded or suspended transition from mid- to late-gestational stages of NPC development, so that hypoxia should confer astrocytic differentiation potential on hNPCs as we observed in mouse mgNPCs. We therefore cultured hPSC-derived hNPCs under hypoxic conditions and found that this is indeed the case. The hNPCs differentiated rapidly (within 4 weeks) into astrocytes, and this was inversely correlated with the methylation status of the *GFAP* promoter. We also show that conferral of astrocytic differentiation potential on the hNPCs is achieved by a collaboration between hypoxia-inducible factor 1α (HIF1α) and Notch signaling. Furthermore, we show that astrocytes derived from RTT-hiPSCs using our method impair aspects of neuronal development such as neurite outgrowth and synaptic formation, indicating that our protocol will accelerate investigations of the functions of neurological disorder-relevant astrocytes in vitro.

RESULTS

Astrocytic Differentiation Potential of hNPCs Is Inversely Correlated with DNA Methylation Status in the *GFAP* Promoter

We first re-examined the differentiation tendencies of four hNPC lines established from hiPSCs (AF22 and AF24), hESCs (AF23) (Falk et al., 2012), and human fetal brain (CB660) (Sun et al., 2008) by immunocytochemistry with antibodies against the neuron and astrocyte markers tubulin β 3 class III (TUBB3) and GFAP, respectively. Whereas fetal brain-derived CB660 could efficiently differentiate into both TUBB3-positive neurons and GFAP-positive astrocytes after a 4-week differentiation period, the astrocyte population was extremely low in AF22 and AF23 (Figures 1A and 1B). Moreover, only a small fraction of AF22 and AF23 differentiated into astrocytes even when stimulated with LIF, which activated STAT3 in these cells (Figures S1A and S1B). Interestingly, AF24 (hNPCs established from CB660-derived hiPSCs) also barely differentiated into astrocytes even in the presence of LIF (Figures 1A, 1B, S1A, and S1B). These results suggest that the capacity to differentiate into astrocytes is restricted in hNPCs if they are derived from hPSCs, regardless of the properties of the original cells. Since it has been shown that mouse mgNPCs have a limited astrocytic differentiation potential due to the hyper-methylation status in astrocytic gene promoters (Namihira et al., 2009; Takizawa et al., 2001), we next examined the methylation status of the *GFAP* promoter as a representative gene promoter in these cells (Figure 1C). Bisulfite sequence analysis revealed a high-methylation status for the *GFAP* promoter in AF22, 23, and 24 but not in CB660 (Figures 1D and 1E). These methylation statuses were inversely correlated with the astrocytic differentiation ability of each cell line (Figures 1B and 1E).

Hypoxia Increases Astrocytic Differentiation of hNPCs in Association with Demethylation of the *GFAP* Promoter

hNPCs with low astrocytic differentiation potential (AF22, 23, and 24) were all established from hPSCs, and had never been exposed to hypoxia during or after their establishment (Falk et al., 2012). In contrast, CB660 hNPCs were prepared directly from a human fetal brain around gestational week 8 (Sun et al., 2008), indicating that they had been under hypoxia until at least this time because embryonic tissues including brain are in hypoxic conditions (Mohyeldin et al., 2010; Simon and Keith, 2008). Since we have previously shown that hypoxia confers astrocytic differentiation potential on mouse mgNPCs (Mutoh et al., 2012), we speculated that the difference in astrocytic differentiation between these hNPCs is attributable to their exposure

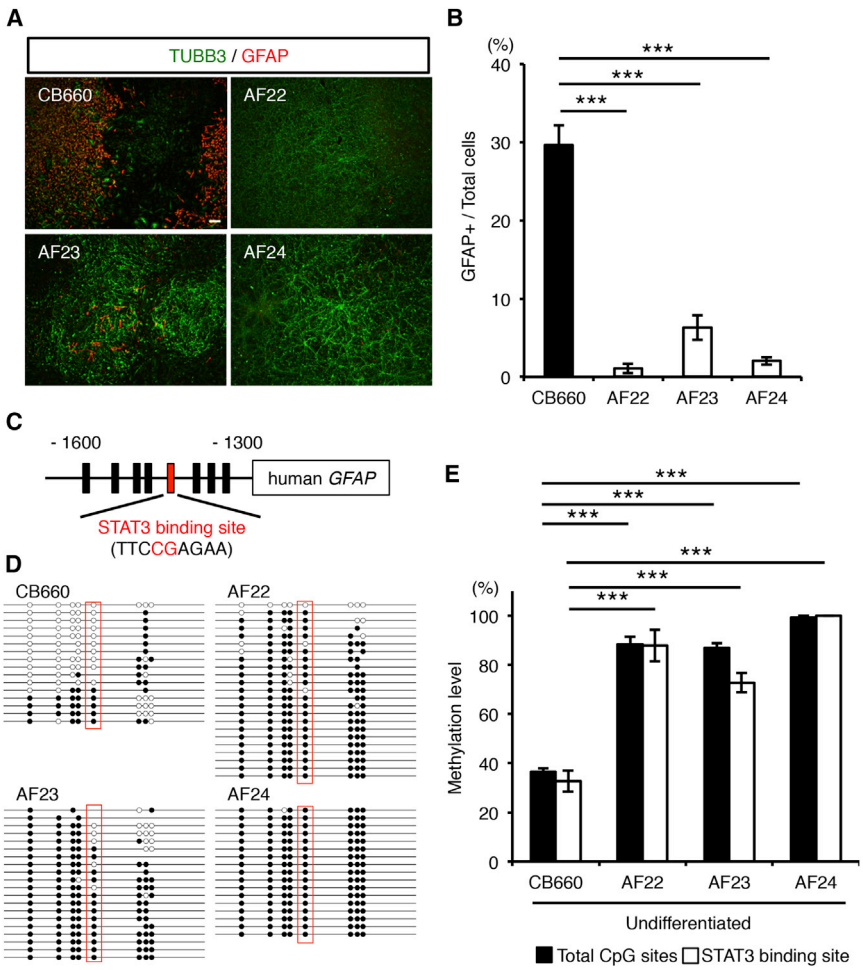

Figure 1. Impairment of Astrocytic Differentiation Is Inversely Correlated with DNA Methylation Level in the *GFAP* Promoter

(A) Representative images of staining for TUBB3 (green) and GFAP (red) after 28 days of differentiation of four hNPCs: CB660 (from fetal brain), AF22 (from hiPSCs established from human adult fibroblasts), AF23 (from hESCs), and AF24 (from iPSCs reprogrammed from CB660). Scale bar, 200 μm.

(B) Quantification of GFAP-positive cells for assessing differentiation of hNPCs in (A).

(C) Diagram showing the human *GFAP* promoter region including the STAT3 recognition site and seven other CpG sites. The red bar of CG dinucleotide indicates a methylation site of STAT3 binding site.

(D) Methylation status of the *GFAP* promoter region in the indicated hNPCs cultured under maintenance conditions. Open and filled circles represent unmethylated and methylated CpG sites, respectively. The red rectangles of CG dinucleotide indicate STAT3 binding sites.

(E) Methylation frequency within the STAT3 binding site and total CpG sites in *GFAP* promoters. Solid bars depict methylation levels in total CpG sites, and white bars depict those in the STAT3 binding site (n = 3 independent experiments; error bars are mean ± SD; ***p < 0.001; one-way ANOVA and Tukey's test). See also Figure S1.

to hypoxia. Therefore, we decided to test whether hypoxic exposure enhances astrocytic differentiation of AF22-24. Since HIF1α, an oxygen sensor, has been shown to be crucial for mouse mgNPCs to acquire astrocytic differentiation ability (Mutoh et al., 2012), we first examined HIF1α expression together with that of HIF2α in our hNPC culture (Figures 2C, 2D, and 2E). Once induced, HIF1α expression was sustained until 28 days (Figures 2D and 2E). qRT-PCR data indicated that *HIF1α* expression peaked at 21 days after the onset of low-oxygen culture (Figure 2E). On the contrary, HIF2α and *HIF2α* expression were induced transiently, but then returned to basal levels (Figures 2D and 2E). These results are inconsistent with those of two previous studies (Forristal et al., 2009; Stacpoole et al., 2011). However, this may be due to differences in cell types and culture conditions: Forristal et al. (2009) performed experiments using hESCs in the maintenance condition, and Stacpoole et al. (2011) did so using hESC-derived NPCs, which were maintained in aggregation form, in spinal motor neuron- and midbrain dopaminergic neuron-inducing conditions, whereas we maintained and differentiated hPCS-derived hNPCs in monolayer. Furthermore, cultures in both of those studies but not in ours contained basic fibroblast growth factor (bFGF), which has a variety of effects on cell behavior. We therefore presume that these discrepancies explain the difference in HIF1α and HIF2α expression between the previous experiments and ours, although we cannot completely exclude other possibilities.

When AF22–24 were cultured under hypoxia, we observed a dramatic induction of GFAP- (Figures 2A and 2B for AF22-24) and aquaporin-4 (AQP4)-positive astrocytes (Figure S2A for AF22) after 28 days of differentiation. In addition to *GFAP* and *AQP4* mRNA expression, we also confirmed the upregulation of expression of another astrocyte-specific gene, aldehyde *dehydrogenase 1 family member L1* (*ALDH1L1*), in AF22 under hypoxia (Figure S2B). Consistent with this observation, DNA methylation in the *GFAP* promoter, including the STAT3 binding site, was greatly reduced in AF22 under hypoxia compared with normoxia after 28 days of differentiation (Figures 2C and 2F). Moreover, mRNA expression of *nuclear factor IA* (*NFIA*) and *hairy and enhancer of split 5* (*HES5*),

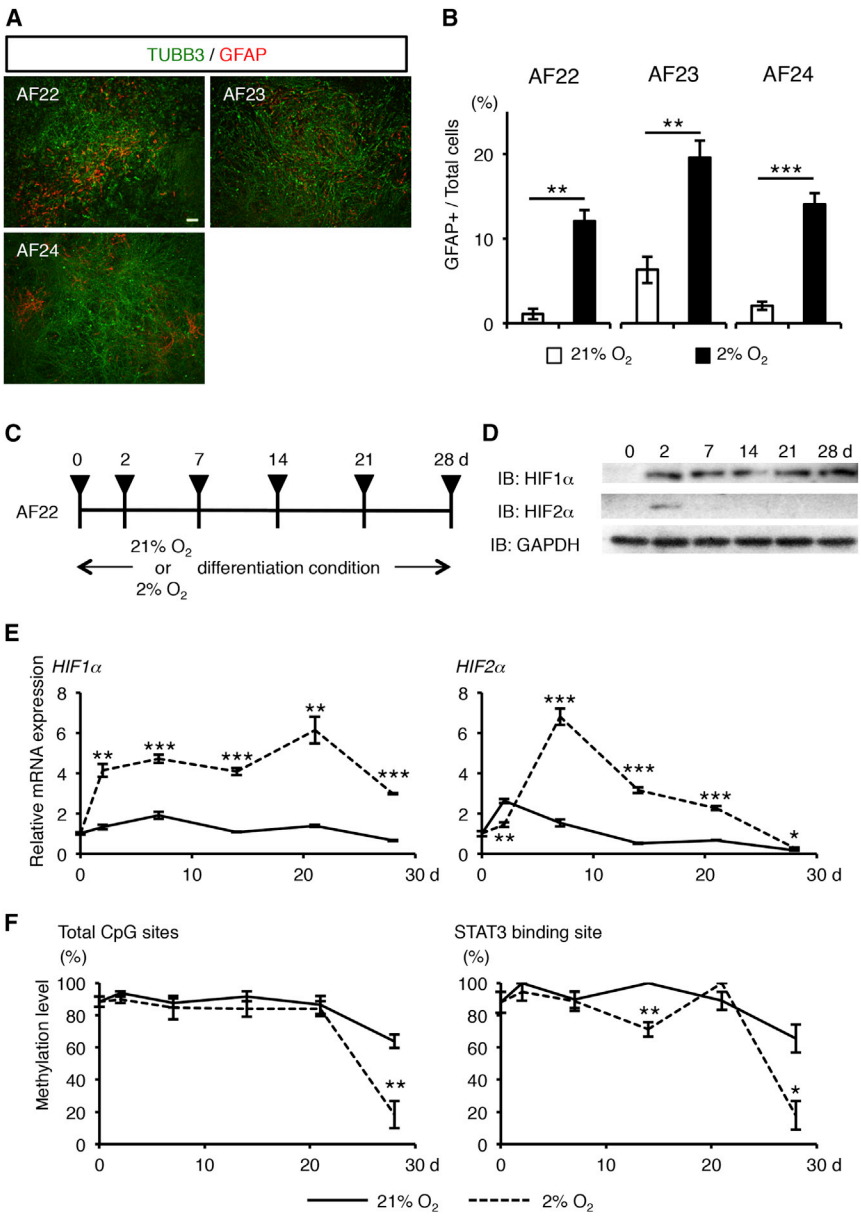

Figure 2. Hypoxia Increases Astrocytic Differentiation of hNPCs via DNA Demethylation

(A) Representative images of staining for TUBB3 (green) and GFAP (red) after 28 days of differentiation of the indicated hNPCs under hypoxia. Scale bar, 200 μm.

(B) Quantification of GFAP-positive cells for assessing differentiation under normoxic or hypoxic conditions of hNPCs (n = 3 independent experiments).

(C) Experimental scheme to examine the expression of HIF1α and HIF2α and methylation status of the *GFAP* promoter during differentiation of AF22 under normoxic or hypoxic conditions. AF22 cells were harvested at the indicated times.

(D) Time-course western blot analysis of HIF1α and HIF2α expression in AF22 under 2% O_2 differentiation conditions. GAPDH was also blotted as a control.

(E) Expression levels of *HIF1α* and *HIF2α* in AF22 in normoxic (solid line) or hypoxic (broken line) differentiation conditions (n = 3 independent experiments).

(F) Methylation frequency within total CpG sites (left panel) and the STAT3 binding site (right panel) in the *GFAP* promoter in normoxic (solid line) or hypoxic (broken line) differentiation conditions (n = 3 independent experiments; error bars are mean ± SD; *p < 0.05, **p < 0.01, ***p < 0.001; Student's *t* test). See also Figure S2.

downstream targets of Notch signaling (Mutoh et al., 2012), was upregulated under the hypoxic condition (Figure S2C). Since Notch signaling is known to be important for mouse mgNPCs to acquire astrocytic differentiation potential by reducing DNA methylation levels in the promoters of astrocyte-specific genes (Namihira et al., 2009), it seemed likely that Notch signaling would also contribute to demethylation of the *GFAP* promoter in the hNPCs under hypoxia. We could detect the expression of at least one astrocyte-inducing factor, *LIF*, in AF22 in the differentiated condition (Figure S2D), suggesting that these cells are in an environment where they can express *GFAP* once the gene promoter has become demethylated. Since we have focused on astrocytic differentiation of hPSC-derived NPCs in this study, we did not extensively investigate their differentiation into oligodendrocytes, which are generated at late-gestational stages in addition to astrocytes. However, although we must await detailed investigations in the future, we did find that the expression of oligodendrocyte-related genes, such as *platelet-derived growth factor receptor β* (*PDGFRβ*), *chondroitin sulfate proteoglycan 4* (*CSPG4*, also known as *NG2*), *2′,3′-cyclic nucleotide 3′ phosphodiesterase* (*CNP*), and *proteolipid protein 1* (*PLP1*), was increased in AF22 under hypoxia compared with normoxia 28 days after the initiation of differentiation (Figure S2E), implying that our low-oxygen culture can

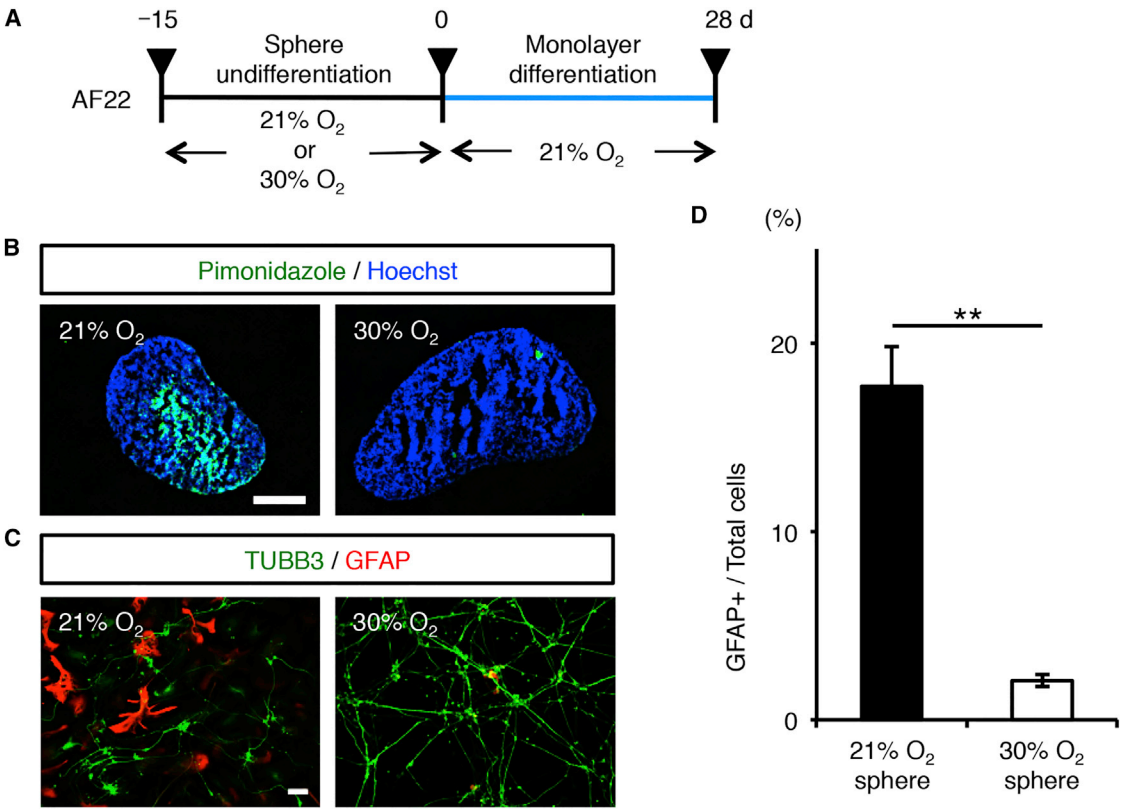

Figure 3. A Hypoxic Environment inside the Aggregation Accounts for Enhanced Astrocytic Differentiation of hNPCs

(A) Experimental scheme for differentiation of AF22 through sphere-forming culture.

(B) Representative images of staining for Hypoxiprobe (pimonidazole adducts, green) and Hoechst (blue) of AF22 cultured in aggregation forms under 21% or 30% O_2 conditions. Pimonidazole adduct formation was clearly observed under 21% but not 30% O_2. Scale bar, 300 μm.

(C) Representative images of staining for TUBB3 (green) and GFAP (red), indicating that efficient GFAP-positive astrocytic differentiation of AF22 was induced through 21% O_2 but not 30% O_2 aggregation culture. Scale bar, 50 μm.

(D) Quantification of GFAP-positive cells cultured as in (C) (n = 3 independent experiments; error bars are mean ± SD; **p < 0.01; Student's *t* test). See also Figure S3.

likewise be applied to monitoring the induction of oligodendrocytic differentiation of hPSC-derived NPCs.

Low Oxygen Level Is Responsible for Aggregation Culture-Mediated Potentiation of hNPCs to Differentiate into Astrocytes

Accumulating evidence suggests that aggregation (or sphere) culture of hNPCs can improve the generation of astrocytes from the cells (Imamura et al., 2015; Lancaster et al., 2013; Taguchi et al., 2014; Volkner et al., 2016). Taking this and our findings above into consideration, we suspected that the reason why aggregation culture can enhance astrocytic differentiation of NPCs is that the cells inside the aggregation are in a hypoxic microenvironment even though the culture itself is conducted at atmospheric oxygen level. To test this, we cultured AF22, which had never or scarcely been cultured in aggregation, for 15 days as spheres under either normoxic (21% O_2) or hyperoxic (30% O_2) in undifferentiated conditions, and then induced their differentiation for 28 days in monolayer culture (Figure 3A). We assessed oxygen levels in the aggregates using a chemical reagent, pimonidazole. Pimonidazole is reductively activated in hypoxic cells and forms stable adducts with sulfhydryl groups in amino acids, at around or below 10 mmHg, which can be detected with specific antibodies (Arteel et al., 1998). As we anticipated, pimonidazole adducts were clearly detected inside the aggregation formed in normoxia but not that in hyperoxia (Figure 3B), indicating that cells within the normoxic aggregation are in a hypoxic environment. We also confirmed that vascular endothelial growth factor, a downstream target of HIF1α, was expressed in the aggregates (Figure S3). Twenty-eight days after differentiation was induced, we could detect efficient GFAP-positive astrocytic differentiation of AF22 that had been cultured as spheres in normoxia but not in hyperoxia (Figures 3A, 3C, and 3D), suggesting that the previously reported

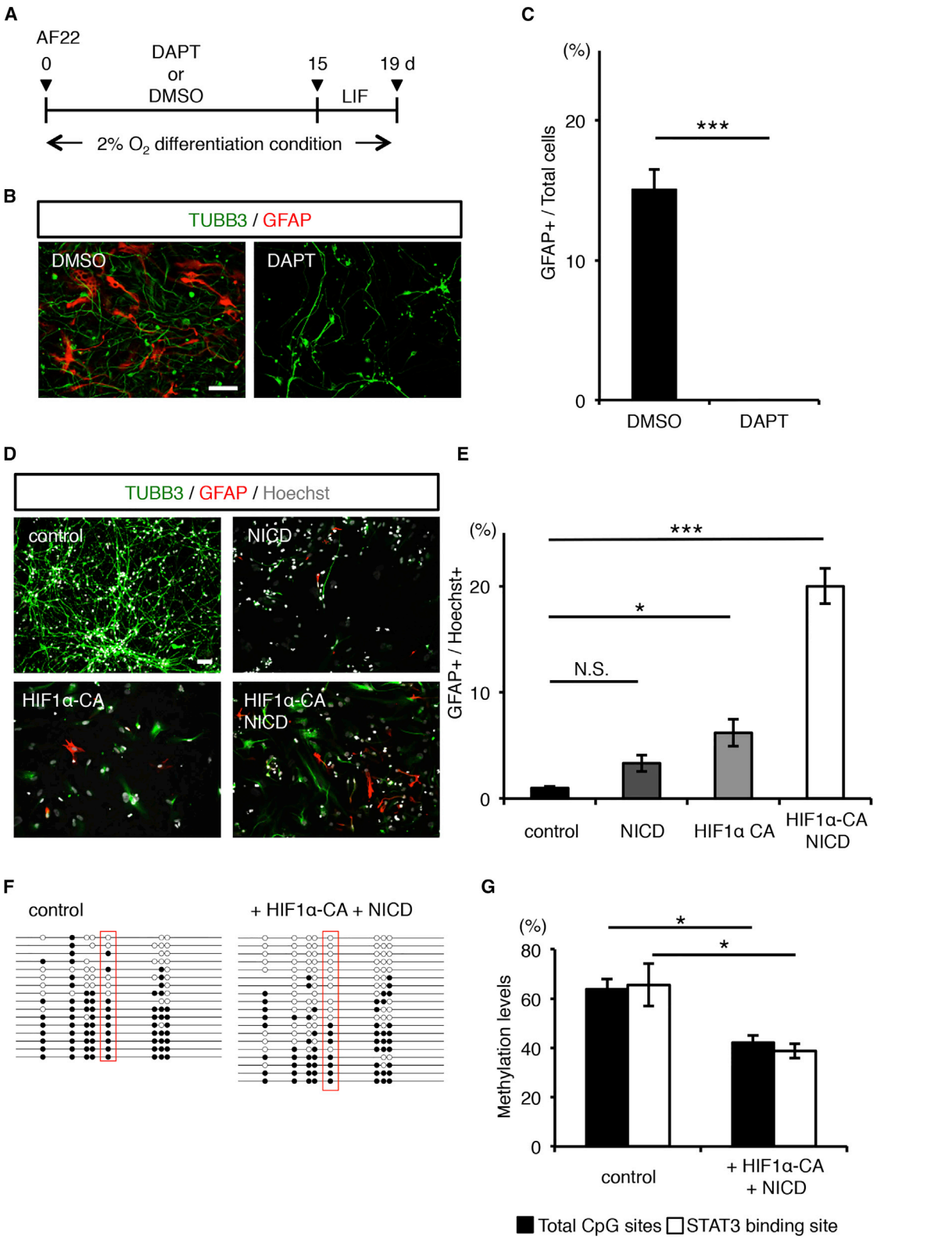

(legend on next page)

potentiation of hNPCs for astrocytic differentiation in sphere culture (Edri et al., 2015) is attributable to low oxygen levels in the aggregates.

Notch Signaling and HIF1α Function Synergistically to Confer Astrocytic Differentiation Potential on hNPCs

Because Notch signaling has been shown to be crucial for mouse mgNPCs to acquire astrocytic differentiation ability (Namihira et al., 2009), we next examined whether this is also the case for hNPCs. AF22 cultured under hypoxia differentiated to GFAP-positive astrocytes in response to LIF stimulation, but did not do so in the presence of a γ-secretase inhibitor (*N*-[*N*-(3,5-difluorophenacetyl)-L-alanyl]-*S*-phenylglycine *t*-butyl ester; DAPT) which is widely used to block Notch signaling (Figures 4A–4C). When we activated Notch signaling by the expression of the Notch intracellular domain (NICD), AF22 showed a slight but not statistically significant increase in astrocytic differentiation in the normoxic culture conditions (Figures 4D and 4E). However, the expression of a constitutively active form of HIF1α (HIF1α-CA) (Yan et al., 2007), to mimic the hypoxic situation in the cells, synergistically induced astrocytic differentiation of AF22 with NICD under normoxia even in the absence of exogenous LIF (Figures 4D and 4E). Consistent with this, simultaneous expression of NICD and HIF1α-CA significantly reduced the methylation level of the *GFAP* promoter (Figures 4F and 4G). Taken together, these data suggest that HIF1α and Notch signaling are cooperatively important for hypoxia-mediated acquisition of astrocytic differentiation potential by hNPCs derived from hPSCs.

Astrocytic Differentiation of hPSC-Derived hNPCs Is Further Increased in the Presence of FBS under 1% O_2 Conditions

Although hypoxia (2% O_2) has been shown to enhance the astrocytic differentiation of hPCS-derived hNPCs, we tried to find more efficient conditions for astrocytic differentiation of these cells. When we cultured AF22 in the presence of fetal bovine serum (FBS) under 1% O_2 hypoxia as indicated in Figure S4A, these cells differentiated to GFAP-positive astrocytes more efficiently than they did under all other conditions examined in this study (Figures S4B and S4C). In addition, we also confirmed the upregulation of *GFAP* and *ALDH1L1* mRNA expression in AF22 under 1% O_2 with FBS (Figure S4D). Although the expression of another astrocytic marker, *AQP4*, was reduced in the presence of FBS compared with the serum-free 2% O_2 condition (Figure S4D), the expression level was still much higher than that in undifferentiated AF22, in accordance with a previous study (Table S2 of Edri et al., 2015), supporting our proposal that this hypoxic condition promotes astrocytic differentiation of hPSC-derived hNPCs.

Functional Analysis of RTT Patient-Derived Astrocytes Generated in Hypoxic Culture

A recent study has shown that RTT-hiPSC-derived astrocytes have adverse effects on the morphology and function of neurons (Williams et al., 2014). In that study, astrocytes were generated from hiPSC-derived hNPCs only after more than 200 days in culture, whereas our hypoxic culture could yield astrocytes from hNPCs within 28 days (Figures 2A and 2B). However, it was unclear whether these astrocytes, generated rapidly through hypoxia, would be functional enough to allow us to investigate pathological aspects of patient-relevant astrocytes.

We have recently established isogenic pairs of either WT or MT *MECP2*-expressing hiPSCs from a 10-year-old RTT patient and converted them into hNPCs (RS2-65M and RS2-62P, respectively) (Andoh-Noda et al., 2015). To obtain RTT patient-derived astrocytes, we cultured RS2-65M and RS2-62P in the presence of FBS under 1% O_2 (Figure 5A). We found that more than 60% of cells differentiated into

Figure 4. Cooperation between Notch Signaling and HIF1α Mediates Astrocytic Differentiation under Hypoxia

(A) Experimental scheme for culturing AF22 to examine the effect of Notch signal activation using DAPT (γ-secretase inhibitor; 10 μM) under the hypoxic differentiation condition.

(B) Representative images of staining for TUBB3 (green) and GFAP (red) 19 days after differentiation under hypoxia in the presence or absence of DAPT. LIF was added to the culture medium for 4 days to stimulate astrocytic differentiation. Scale bar, 50 μm.

(C) Quantification of GFAP-positive cells for assessing the effect of Notch signaling (n = 3 independent experiments; Student's *t* test).

(D) Representative images of staining for TUBB3 (green) and GFAP (red) at 28 days after overexpression of NICD with or without HIF1α-CA expression under the normoxic differentiation condition. Nuclei were counterstained with Hoechst (gray). Scale bar, 50 μm.

(E) Quantification of GFAP-positive cells for assessing differentiation of hNPCs in (D) (n = 4 independent experiments; one-way ANOVA and Tukey's test).

(F) Methylation status of the *GFAP* promoter in AF22 (left) and in AF22 expressing HIF1α-CA and NICD (right), after 28 days of differentiation. Open and filled circles represent unmethylated and methylated CpG sites, respectively. The red bar of CG dinucleotide indicates a methylation site of STAT3 binding site.

(G) Methylation frequency within the STAT3 binding site and total CpG sites in the *GFAP* promoter in (F). Solid bars depict methylation levels in total CpG sites, and white bars depict that in the STAT3 binding site (n = 3 independent experiments; error bars are mean ± SD; N.S., not statistically significant, *p < 0.05, ***p < 0.001; Student's *t* test).

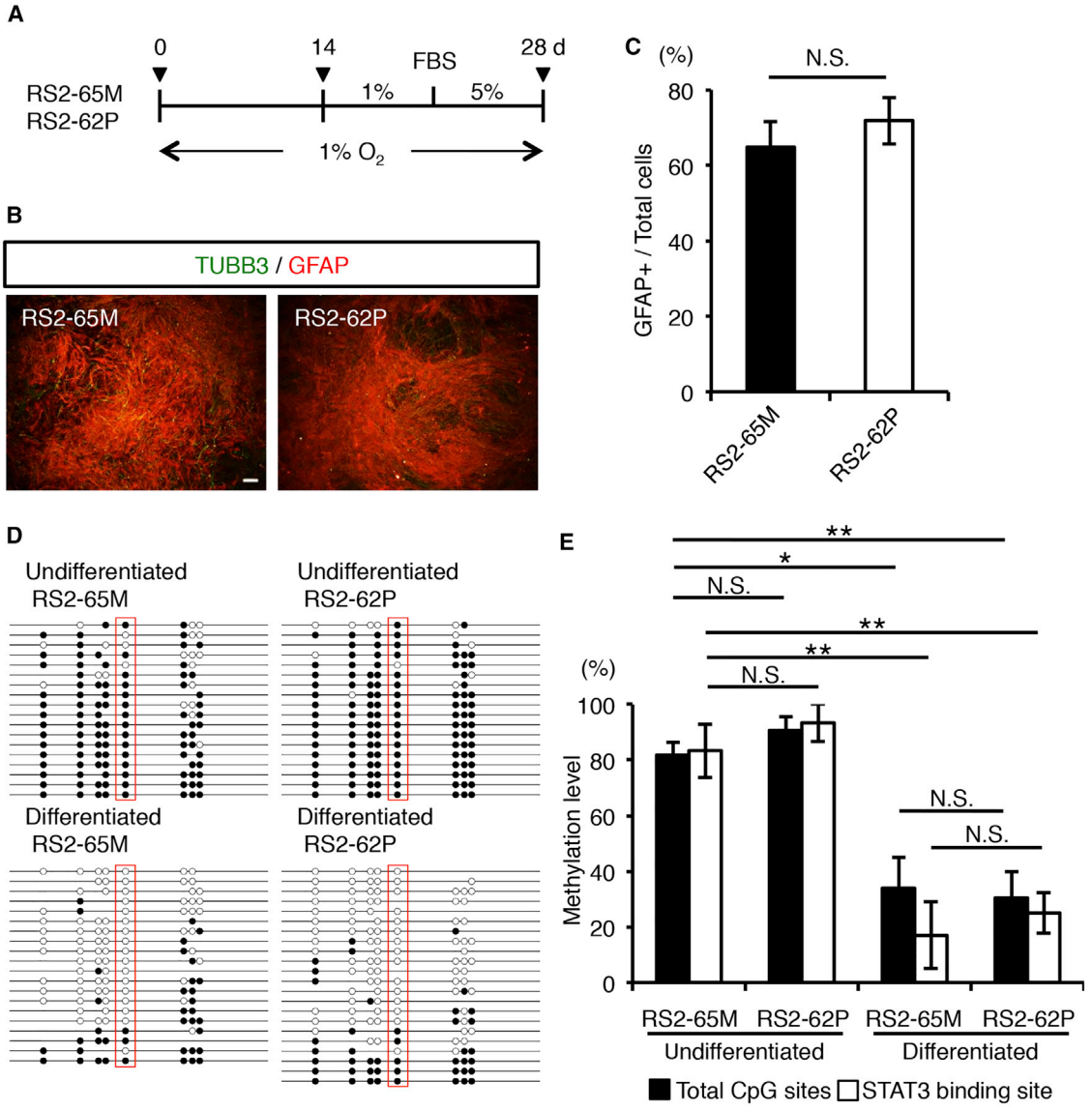

Figure 5. Hypoxia Enables RTT Patient-Derived hNPCs to Rapidly Differentiate into Astrocytes

(A) Schematic representation of the protocol for generating astrocytes from RS2-65M and -62P.

(B) Representative images of staining for TUBB3 (green) and GFAP (red) after 28 days of astrocytic differentiation of RS2-65M and -62P hNPCs. Scale bar, 200 μm.

(C) Quantification of GFAP-positive cells in (B) for assessing differentiation of hNPCs (n = 3 independent experiments; Student's *t* test).

(D) Methylation status of the *GFAP* promoter region in RS2-65M and -62P cultured in undifferentiated or differentiated conditions as in (A). Open and filled circles represent unmethylated and methylated CpG sites, respectively. The red bar of CG dinucleotide indicates a methylation site of STAT3 binding site.

(E) Methylation frequency within the STAT3 binding site and total CpG sites in the *GFAP* promoter in (D). Solid bars depict methylation levels in total CpG sites, and white bars depict those in the STAT3 binding site (n = 3 independent experiments; error bars are mean ± SD; N.S., not statistically significant, *p < 0.05, **p < 0.01; one-way ANOVA and Tukey's test). See also Figure S4.

astrocytes in both cell lines after 28 days of differentiation (Figures 5B and 5C). In addition, bisulfite sequence analysis revealed that hypoxia reduced DNA methylation in the *GFAP* promoter, including the STAT3 binding site, in both cells (Figures 5D and 5E).

To confirm previously reported effects of RTT patient-derived astrocytes on soma size and neurite outgrowth of neurons, we co-cultured hNPCs (AF22) in normoxia with WT or MT *MECP2*-expressing astrocyte-enriched cells generated under hypoxia from RS2-65M or RS2-62P,

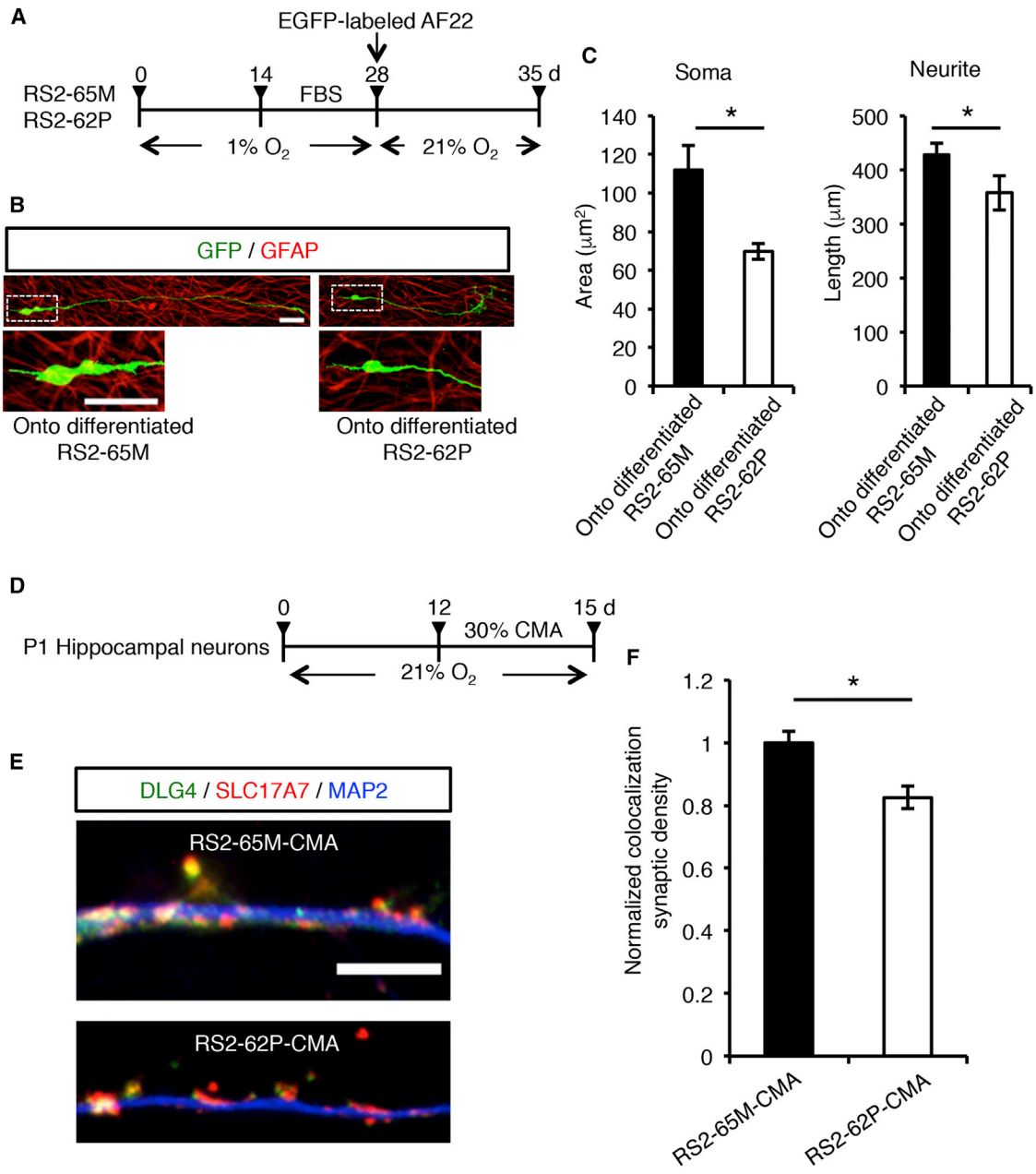

Figure 6. Astrocytes Derived from RTT-hiPSCs Impair Neuronal Maturation

(A) Experimental scheme for assessing soma size and neurite length in EGFP-labeled AF22 with neuronal morphology. Astrocytic differentiation was induced in RS2-65M or -62P with FBS (from day 14 to 28) under hypoxia (1% O_2). EGFP-labeled AF22 were then seeded onto these differentiated astrocytes and cultured under normoxia in the absence of FBS for 7 days.

(B) Representative images of staining for EGFP (green) and GFAP (red) of AF22 after 7 days of co-culture with differentiated RS2-65M or -62P (more than 60% of these cells differentiated into astrocytes; see also Figure 5). Boxed areas in the upper images are enlarged below. Scale bar, 20 μm.

(C) Quantification of soma area and neurite length of EGFP-labeled AF22 with neuronal morphology after 7 days of co-culture with differentiated RS2-65M or -62P (n = 3 independent experiments).

(D) Experimental scheme for neuronal culture with conditioned medium of astrocyte-enriched cells (CMA) collected from differentiated RS2-65M or -62P, which were cultured as in Figure 5. Each CMA was added to neuronal culture as 30% of the medium volume at day 12 and the neurons were cultured for an additional 3 days.

(legend continued on next page)

respectively (Figure 6A). After 7 days of co-culture, over 70% of AF22 became TUBB3-positive cells displaying neuronal morphology on both WT and MT *MECP2*-expressing astrocyte-enriched cells, indicating that hNPCs differentiated into neurons efficiently regardless of the genotype of the astrocytes (data not shown). We found that soma size and neurite length of cells with neuronal morphology were reduced, as reported previously (Williams et al., 2014), when the cells were co-cultured with MT *MECP2*-expressing astrocyte-enriched cells compared with those observed in the co-culture with WT *MECP2*-expressing cells (Figures 6B and 6C).

A previous study has shown that hippocampal neurons have lower spine density in RTT patients than in healthy individuals (Chapleau et al., 2009). However, it remains unknown whether astrocytes with MT *MECP2* expression contribute to this phenotype. To address this question, we cultured WT mouse hippocampal neurons with conditioned medium of astrocyte-enriched cells (CMA) from WT or MT *MECP2*-expressing cells generated from hNPCs as in Figure 6A (Figure 6D), and co-immunostained these neurons with antibodies against discs large MAGUK scaffold protein 4 (DLG4, also known as post-synaptic density protein 95 (PSD-95)) and solute carrier family 17 menber 7 (SLC17A7, also known as vesicular glutamate transporter 1 (VGLUT1)), which are post- and pre-synaptic markers, respectively. We observed that treatment of neurons with CMA from MT *MECP2*-expressing cells suppressed synaptic formation (Figures 6E and 6F), raising the possibility that MT *MECP2*-expressing astrocytes indeed contribute to the dysregulation of synaptic (or spine) formation reported in RTT patients.

DISCUSSION

With the advent of hESCs (Thomson et al., 1998) and hiPSCs (Takahashi et al., 2007; Yu et al., 2007), our understanding of mechanisms underlying phenomena such as cellular dysfunction in neurological diseases has advanced greatly because these hPSCs are, at least in part, capable of recapitulating development and disease phenotypes in culture (Sanchez-Danes et al., 2012). However, these studies have mainly focused on neuronal functions and not on the roles of astrocytes, even though astrocytes are known to participate in various types of neurological disorders (Allen et al., 2012; Christopherson et al., 2005; Hamilton and Attwell, 2010; Haydon and Nedergaard, 2015; Kucukdereli et al., 2011; Molofsky et al., 2012; Ullian et al., 2001; Zhang et al., 2016). One of the reasons for this discrepancy is that generating neurons from hPC-derived hNPCs is relatively easy, whereas generating astrocytes is extremely time consuming (Edri et al., 2015; Kondo et al., 2013; Krencik et al., 2011; Williams et al., 2014). In the mammalian CNS, astrocytes are known to be produced from NPCs at the late-gestational stage during development, and mounting evidence has indicated that this stage-dependent generation of astrocytes from NPCs is achieved by systematic cooperation between environmental cues and cell-intrinsic programs. In this context, we have previously shown that the retarded acquisition of astrocytic differentiation potential by mouse mgNPCs cultured in vitro is due to the high oxygen levels compared with those encountered in vivo (Mutoh et al., 2012), leading us to hypothesize that low oxygen level confers astrocytic differentiation potential on hPSC-derived hNPCs. Consistent with our previous study in the mouse, recent work has suggested that hypoxia mediates the potentiation of astrocytic differentiation in hNPCs (Patterson et al., 2014; Xie et al., 2014). In these papers, the microRNA let-7b was reported to enhance astrocyte generation from hNPCs under hypoxia. let-7b has subsequently been proposed to promote astrocytic differentiation of mouse NPCs in parallel with JAK-STAT signaling (Shenoy et al., 2015). In the present study, we have verified a mechanism for potentiating hPSC-derived hNPCs to differentiate into astrocytes: low oxygen levels confer astrocytic differentiation potential on hNPCs through a collaboration between HIF1α and Notch signaling, which leads to demethylation of the astrocyte-specific gene *GFAP*.

Regarding mouse mgNPCs, we have previously indicated that Notch signal activation in NPCs induces the expression of nuclear factor IA (Nfia), which binds to astrocyte-specific gene promoters, resulting in dissociation of the maintenance DNA methyltransferase 1 (Dnmt1) from the promoters (Namihira et al., 2009). Dnmt1 dissociation eventually leads to demethylation of astrocyte-specific gene promoters as NPCs continue to divide, thereby conferring astrocytic differentiation capacity on mouse NPCs (Namihira et al., 2009). Demethylation of astrocyte-specific gene promoters was further enhanced when mouse NPCs were cultured under in vivo-mimicking hypoxic conditions, most likely because HIF1α physically interacts with NICD to effectively induce a Notch signal target gene, *Nfia*

(E) Neurites of mouse hippocampal neurons were immunostained for DLG4 (green), SLC17A7 (red), and MAP2 (blue) after 3 days of culture with CMA from differentiated RS2-65M or -62P. Representative images are shown. Scale bar, 10 μm.
(F) Quantification of co-localized DLG4 and SLC17A7 signals in (E) for assessing normalized synaptic densities (n = 3 independent experiments; 30 neurons in each sample; error bars are mean ± SD; *p < 0.05; Student's *t* test).

(Gustafsson et al., 2005; Namihira et al., 2009). In the present study, although we have revealed that the expression of Notch signal target genes including *NFIA* was upregulated, and that HIF1α cooperated with Notch signaling to control astrocytic differentiation of hNPCs under hypoxia as occurs in mouse NPCs, to elucidate whether hNPCs exploit exactly the same mechanism as mouse NPCs must await future investigation.

DNA methylation in the *GFAP* promoter, including the STAT3 binding site, decreased gradually, and a substantial difference was observed in AF22 between 2% and 21% O_2 conditions 28 days after the induction of differentiation. There are several possible reasons why it took a relatively long time to see this methylation difference between 2% and 21% O_2 conditions: (1) some time was required for the relevant factor genes to be transcribed, translated into protein, and to accumulate sufficiently to function efficiently; (2) as we have shown in the present and a previous study (Namihira et al., 2009), Notch signaling in NPCs must be activated to induce DNA demethylation in astrocytic gene promoters. Notch ligands are expressed in immature neurons, which are generated from NPCs, and these immature neurons are produced only from around 10 days after the initiation of differentiation (hNPCs need more time than rodent NPCs before neuronal differentiation can be detected); and, finally, (3) demethylation of astrocytic gene promoters is mediated by a passive demethylation process that requires DNA replication during cell division, meaning that this demethylation does not occur immediately after the demethylation-related factor Nfia, which induces dissociation of Dnmt1 from astrocytic gene promoters, is produced by Notch signal activation in NPCs (Namihira et al., 2009). Determining the precise cause of this time lag remains an important challenge for future studies.

Here, using hNPCs derived from RTT patient iPSCs as an example, we have shown that our method of hypoxia-mediated rapid astrocytic differentiation of hNPCs can be applied to functional analysis of patient-derived astrocytes. We revealed that *MECP2* MT astrocytes diminish the soma size, neurite outgrowth, and synaptic formation of neurons. As well as in RTT, astrocyte dysfunction has also been implicated in many other neurological diseases such as Alexander disease, which is characterized by genetic mutations in *GFAP* (Hagemann et al., 2013). Several types of transgenic mice with mutations in *GFAP* have been established. However, not all of the human pathological phenotypes of astrocytes can be reproduced in mice, necessitating research using human astrocytes, and this holds true for other astrocyte-mediated neurological disorders. Our hypoxic culture greatly accelerates the production of patient-relevant astrocytes, bringing us one step closer to better understanding the mechanisms underlying these disorders and also paving the way for development of strategies for their treatment.

EXPERIMENTAL PROCEDURES

Cell Culture

Four hNPC lines, AF22 (58 passages), AF23 (29 passages), AF24 (21 passages), and CB660 (33 passages), were established and maintained in monolayer culture as described previously (Falk et al., 2012; Sun et al., 2008). Isogenic pairs of either WT or MT *MECP2*-expressing hNPCs derived from RTT patient iPSCs (RS2-65M [11 passages] and RS2-62P [10 passages]) (Andoh-Noda et al., 2015) were established and maintained briefly in sphere culture (fewer than 10 passages), and then maintained in monolayer culture. All of these cells were plated onto 0.1 mg/mL poly-L-ornithine (Sigma)- and 10 μg/mL laminin (Corning)-coated plates in maintenance medium: DMEM/F12 (Invitrogen), 0.1 mg/mL penicillin/streptomycin (Nacalai Tesque), 1 μL/mL B27 (Gibco), 10 ng/mL bFGF (PeproTech), and 10 ng/mL epidermal growth factor (EGF, PeproTech). Cells were passaged at a ratio of 1:3 every third to fourth day using TrypLE (Gibco). To induce differentiation, cells were plated onto Matrigel (Corning)-coated 35-mm dishes at a density of 0.5–1.0 × 10^5 cells/dish in maintenance medium lacking both EGF and bFGF (differentiation medium), and then cultured in either normoxic (21% O_2) or hypoxic (2% O_2) conditions. Half of the medium was changed every 2 days. LIF (1/1,000; Wako) was employed for further induction of astrocytes. To inhibit Notch signaling, DAPT (EMD Millipore) was added to the differentiation medium.

To induce astrocytic differentiation more efficiently, hNPCs established from hPSCs were cultured in differentiation medium under hypoxia (1% O_2) for 14 days without FBS (Gibco), and then for 7 days each with 1% and 5% FBS.

To obtain CMA, astrocyte-enriched cells differentiated from RS2-65M or RS2-62P were washed with PBS, and the medium was replaced with neuronal medium (Neurobasal Medium; Gibco) supplemented with B27. On the next day, CMA was collected from the culture dishes and added to cultured hippocampal neurons to examine synaptic density.

Neuronal cultures were prepared from P1 mouse hippocampus according to a previously described protocol (Tsujimura et al., 2015), with some modification. In brief, the hippocampus was digested with papain at 37°C for 20 min and triturated with a 1-mL pipette. Minimum essential medium with 5% FBS and 0.6% glucose was added and the mixture was plated onto a poly-L-lysine-coated 35-mm culture dish. After 3 hr, the medium was replaced with maintenance medium supplemented with B27 (Gibco) containing cytosine β-D-arabinofuranoside (5 mM; Sigma) to eliminate proliferating cells. To avoid neuronal cell death by a complete medium change, half of the medium was replaced every 3 days with fresh maintenance medium. After 12 days, the neurons were used for assays.

The study protocol was reviewed and approved by Kyushu University Institutional Review Board for Clinical Research (Approval No. 27-59).

Bisulfite Sequencing

Genomic DNA was extracted and subjected to bisulfite sequencing as described previously (Takizawa et al., 2001). Specific DNA fragments were amplified by PCR using primers described previously

(Namihira et al., 2009; Takizawa et al., 2001). The PCR products were cloned into pGEM-T Easy vector (Promega), and 15 randomly picked clones from three samples were sequenced. Primer sequences for PCRs are available upon request.

Lentivirus Production

A human HIF1α-CA (Addgene) sequence was cloned into pSLIK-Neo vector (Addgene). Tet-O-FUW-hNICD was purchased (Addgene). To prepare lentivirus, HEK293T cells were co-transfected with these constructs and lentiviral packaging vectors (pCAG-HIVgp and pCMV-VSV-G-RSV-Rev). The culture supernatants were collected 48 hr after transfection, and virus was introduced into AF22 by adding the supernatants to the culture medium. HIF1α-CA-expressing cells were purified by G418 (Nacalai Tesque).

Statistical Analysis

Statistical analyses were performed using either Student's *t* test (for comparisons between two groups) or one-way ANOVA (with Tukey's multiple comparison test or Dunnett's post-test) (for multiple groups comparison). All experiments were independently replicated at least three times. Differences were considered statistically significant at $P < 0.05$.

SUPPLEMENTAL INFORMATION

Supplemental Information includes Supplemental Experimental Procedures, four figures, and two tables and can be found with this article online at http://dx.doi.org/10.1016/j.stemcr.2017.05.001.

AUTHOR CONTRIBUTIONS

T.Y., H.N., T.M., H.O., and K.N. designed the study and wrote the manuscript. T.Y., N.U., and H.N. performed the experiments and analyzed the data. All authors discussed the results and commented on the manuscript. K.N. provided funding and supervised the project.

ACKNOWLEDGMENTS

We appreciate the technical assistance from The Research Support Center, Research Center for Human Disease Modeling, Kyushu University Graduate School of Medical Sciences. We have greatly benefited from discussions with J. Kohyama, S. Katada, and T. Imamura. We thank A. Smith for providing the human NPCs (CB660, AF22-24), and I. Smith for editing the manuscript. This work was supported by grants from the Japan Agency for Medical Research and Development, Core Research for Evolutional Science and Technology (AMED-CREST), JSPS KAKENHI (15K14452), MEXT KAKENHI (16H06527), and the Uehara Memorial Foundation to K.N.

Received: September 23, 2016
Revised: May 1, 2017
Accepted: May 1, 2017
Published: June 6, 2017

REFERENCES

Allen, N.J., and Barres, B.A. (2009). Glia - more than just brain glue. Nature *457*, 675–677.

Allen, N.J., Bennett, M.L., Foo, L.C., Wang, G.X., Chakraborty, C., Smith, S.J., and Barres, B.A. (2012). Astrocyte glypicans 4 and 6 promote formation of excitatory synapses via GluA1 AMPA receptors. Nature *486*, 410–414.

Amir, R.E., Van den Veyver, I.B., Wan, M., Tran, C.Q., Francke, U., Zoghbi, H.Y., and Zoghbi, H.Y. (1999). Rett syndrome is caused by mutations in X-linked MECP2, encoding methyl-CpG-binding protein 2. Nat. Genet. *23*, 185–188.

Andoh-Noda, T., Akamatsu, W., Miyake, K., Matsumoto, T., Yamaguchi, R., Sanosaka, T., Okada, Y., Kobayashi, T., Ohyama, M., Nakashima, K., et al. (2015). Differentiation of multipotent neural stem cells derived from Rett syndrome patients is biased toward the astrocytic lineage. Mol. Brain *8*, 31.

Arteel, G.E., Thurman, R.G., and Raleigh, J.A. (1998). Reductive metabolism of the hypoxia marker pimonidazole is regulated by oxygen tension independent of the pyridine nucleotide redox state. Eur. J. Biochem. *253*, 743–750.

Bienvenu, T., and Chelly, J. (2006). Molecular genetics of Rett syndrome: when DNA methylation goes unrecognized. Nat. Rev. Genet. *7*, 415–426.

Bonni, A., Sun, Y., Nadal-Vicens, M., Bhatt, A., Frank, D.A., Rozovsky, I., Stahl, N., Yancopoulos, G.D., and Greenberg, M.E. (1997). Regulation of gliogenesis in the central nervous system by the JAK-STAT signaling pathway. Science *278*, 477–483.

Chapleau, C.A., Calfa, G.D., Lane, M.C., Albertson, A.J., Larimore, J.L., Kudo, S., Armstrong, D.L., Percy, A.K., and Pozzo-Miller, L. (2009). Dendritic spine pathologies in hippocampal pyramidal neurons from Rett syndrome brain and after expression of Rett-associated MECP2 mutations. Neurobiol. Dis. *35*, 219–233.

Christopherson, K.S., Ullian, E.M., Stokes, C.C., Mullowney, C.E., Hell, J.W., Agah, A., Lawler, J., Mosher, D.F., Bornstein, P., and Barres, B.A. (2005). Thrombospondins are astrocyte-secreted proteins that promote CNS synaptogenesis. Cell *120*, 421–433.

Edri, R., Yaffe, Y., Ziller, M.J., Mutukula, N., Volkman, R., David, E., Jacob-Hirsch, J., Malcov, H., Levy, C., Rechavi, G., et al. (2015). Analysing human neural stem cell ontogeny by consecutive isolation of Notch active neural progenitors. Nat. Commun. *6*, 6500.

Falk, A., Koch, P., Kesavan, J., Takashima, Y., Ladewig, J., Alexander, M., Wiskow, O., Tailor, J., Trotter, M., Pollard, S., et al. (2012). Capture of neuroepithelial-like stem cells from pluripotent stem cells provides a versatile system for in vitro production of human neurons. PLoS One *7*, e29597.

Fan, G., Martinowich, K., Chin, M.H., He, F., Fouse, S.D., Hutnick, L., Hattori, D., Ge, W., Shen, Y., Wu, H., et al. (2005). DNA methylation controls the timing of astrogliogenesis through regulation of JAK-STAT signaling. Development *132*, 3345–3356.

Forristal, C.E., Wright, K.L., Hanley, N.A., Oreffo, R.O.C., and Houghton, F.D. (2009). Hypoxia inducible factors regulate pluripotency and proliferation in human embryonic stem cells cultured at reduced oxygen tensions. Reproduction *139*, 85–97.

Gustafsson, M.V., Zheng, X., Pereira, T., Gradin, K., Jin, S., Lundkvist, J., Ruas, J.L., Poellinger, L., Lendahl, U., and Bondesson, M. (2005). Hypoxia requires notch signaling to maintain the undifferentiated cell state. Dev. Cell *9*, 617–628.

Hagemann, T.L., Paylor, R., and Messing, A. (2013). Deficits in adult neurogenesis, contextual fear conditioning, and spatial learning in a Gfap mutant mouse model of Alexander disease. J. Neurosci. *33*, 18698–18706.

Hamilton, N.B., and Attwell, D. (2010). Do astrocytes really exocytose neurotransmitters? Nat. Rev. Neurosci. *11*, 227–238.

Haydon, P.G., and Nedergaard, M. (2015). How do astrocytes participate in neural plasticity? Cold Spring Harb. Perspect. Biol. *7*, a020438.

Hu, B.Y., Weick, J.P., Yu, J., Ma, L.X., Zhang, X.Q., Thomson, J.A., and Zhang, S.C. (2010). Neural differentiation of human induced pluripotent stem cells follows developmental principles but with variable potency. Proc. Natl. Acad. Sci. USA *107*, 4335–4340.

Imamura, Y., Mukohara, T., Shimono, Y., Funakoshi, Y., Chayahara, N., Toyoda, M., Kiyota, N., Takao, S., Kono, S., Nakatsura, T., et al. (2015). Comparison of 2D- and 3D-culture models as drug-testing platforms in breast cancer. Oncol. Rep. *33*, 1837–1843.

Israel, M.A., Yuan, S.H., Bardy, C., Reyna, S.M., Mu, Y., Herrera, C., Hefferan, M.P., Van Gorp, S., Nazor, K.L., Boscolo, F.S., et al. (2012). Probing sporadic and familial Alzheimer's disease using induced pluripotent stem cells. Nature *482*, 216–220.

Kondo, T., Asai, M., Tsukita, K., Kutoku, Y., Ohsawa, Y., Sunada, Y., Imamura, K., Egawa, N., Yahata, N., Okita, K., et al. (2013). Modeling Alzheimer's disease with iPSCs reveals stress phenotypes associated with intracellular Abeta and differential drug responsiveness. Cell Stem Cell *12*, 487–496.

Krencik, R., Weick, J.P., Liu, Y., Zhang, Z.J., and Zhang, S.C. (2011). Specification of transplantable astroglial subtypes from human pluripotent stem cells. Nat. Biotechnol. *29*, 528–534.

Kucukdereli, H., Allen, N.J., Lee, A.T., Feng, A., Ozlu, M.I., Conatser, L.M., Chakraborty, C., Workman, G., Weaver, M., Sage, E.H., et al. (2011). Control of excitatory CNS synaptogenesis by astrocyte-secreted proteins Hevin and SPARC. Proc. Natl. Acad. Sci. USA *108*, E440–E449.

Lancaster, M.A., Renner, M., Martin, C.A., Wenzel, D., Bicknell, L.S., Hurles, M.E., Homfray, T., Penninger, J.M., Jackson, A.P., and Knoblich, J.A. (2013). Cerebral organoids model human brain development and microcephaly. Nature *501*, 373–379.

Marchetto, M.C., Brennand, K.J., Boyer, L.F., and Gage, F.H. (2011). Induced pluripotent stem cells (iPSCs) and neurological disease modeling: progress and promises. Hum. Mol. Genet. *20*, R109–R115.

Mohyeldin, A., Garzon-Muvdi, T., and Quinones-Hinojosa, A. (2010). Oxygen in stem cell biology: a critical component of the stem cell niche. Cell Stem Cell *7*, 150–161.

Molofsky, A.V., Krencik, R., Ullian, E.M., Tsai, H.H., Deneen, B., Richardson, W.D., Barres, B.A., and Rowitch, D.H. (2012). Astrocytes and disease: a neurodevelopmental perspective. Genes Dev. *26*, 891–907.

Mutoh, T., Sanosaka, T., Ito, K., and Nakashima, K. (2012). Oxygen levels epigenetically regulate fate switching of neural precursor cells via hypoxia-inducible factor 1alpha-notch signal interaction in the developing brain. Stem Cells *30*, 561–569.

Nakashima, K., Yanagisawa, M., Arakawa, H., Kimura, N., Hisatsune, T., Kawabata, M., Miyazono, K., and Taga, T. (1999). Synergistic signaling in fetal brain by STAT3-Smad1 complex bridged by p300. Science *284*, 479–482.

Namihira, M., and Nakashima, K. (2013). Mechanisms of astrocytogenesis in the mammalian brain. Curr. Opin. Neurobiol. *23*, 921–927.

Namihira, M., Kohyama, J., Semi, K., Sanosaka, T., Deneen, B., Taga, T., and Nakashima, K. (2009). Committed neuronal precursors confer astrocytic potential on residual neural precursor cells. Dev. Cell *16*, 245–255.

Park, I.H., Arora, N., Huo, H., Maherali, N., Ahfeldt, T., Shimamura, A., Lensch, M.W., Cowan, C., Hochedlinger, K., and Daley, G.Q. (2008). Disease-specific induced pluripotent stem cells. Cell *134*, 877–886.

Patterson, M., Gaeta, X., Loo, K., Edwards, M., Smale, S., Cinkornpumin, J., Xie, Y., Listgarten, J., Azghadi, S., Douglass, S.M., et al. (2014). let-7 miRNAs can act through Notch to regulate human gliogenesis. Stem Cell Rep. *3*, 758–773.

Sanchez-Danes, A., Richaud-Patin, Y., Carballo-Carbajal, I., Jimenez-Delgado, S., Caig, C., Mora, S., Di Guglielmo, C., Ezquerra, M., Patel, B., Giralt, A., et al. (2012). Disease-specific phenotypes in dopamine neurons from human iPS-based models of genetic and sporadic Parkinson's disease. EMBO Mol. Med. *4*, 380–395.

Shenoy, A., Danial, M., and Blelloch, R.H. (2015). Let-7 and miR-125 cooperate to prime progenitors for astrogliogenesis. EMBO J. *34*, 1180–1194.

Simon, M.C., and Keith, B. (2008). The role of oxygen availability in embryonic development and stem cell function. Nat. Rev. Mol. Cell Biol. *9*, 285–296.

Stacpoole, S.R., Bilican, B., Webber, D.J., Luzhynskaya, A., He, X.L., Compston, A., Karadottir, R., Franklin, R.J., and Chandran, S. (2011). Efficient derivation of NPCs, spinal motor neurons and midbrain dopaminergic neurons from hESCs at 3% oxygen. Nat. Protoc. *6*, 1229–1240.

Sun, Y., Pollard, S., Conti, L., Toselli, M., Biella, G., Parkin, G., Willatt, L., Falk, A., Cattaneo, E., and Smith, A. (2008). Long-term tripotent differentiation capacity of human neural stem (NS) cells in adherent culture. Mol. Cell Neurosci. *38*, 245–258.

Svendsen, C.N., ter Borg, M.G., Armstrong, R.J., Armstrong, R.J., Rosser, A.E., Chandran, S., Ostenfeld, T., and Caldwell, M.A. (1998). A new method for the rapid and long term growth of human neural precursor cells. J. Neurosci. Methods *85*, 141–152.

Taguchi, A., Kaku, Y., Ohmori, T., Sharmin, S., Ogawa, M., Sasaki, H., and Nishinakamura, R. (2014). Redefining the in vivo origin of metanephric nephron progenitors enables generation of complex kidney structures from pluripotent stem cells. Cell Stem Cell *14*, 53–67.

Takahashi, K., Tanabe, K., Ohnuki, M., Narita, M., Ichisaka, T., Tomoda, K., and Yamanaka, S. (2007). Induction of pluripotent stem cells from adult human fibroblasts by defined factors. Cell *131*, 861–872.

Takizawa, T., Nakashima, K., Namihira, M., Ochiai, W., Uemura, A., Yanagisawa, M., Fujita, N., Nakao, M., and Taga, T. (2001). DNA

methylation is a critical cell-intrinsic determinant of astrocyte differentiation in the fetal brain. Dev. Cell *1*, 749–758.

Thomson, J.A., Itskovitz-Eldor, J., Shapiro, S.S., Waknitz, M.A., Swiergiel, J.J., Marshall, V.S., and Jones, J.M. (1998). Embryonic stem cell lines derived from human blastocysts. Science *282*, 1145–1147.

Tsujimura, K., Irie, K., Nakashima, H., Egashira, Y., Fukao, Y., Fujiwara, M., Itoh, M., Uesaka, M., Imamura, T., Nakahata, Y., et al. (2015). miR-199a Links MeCP2 with mTOR signaling and its dysregulation leads to Rett syndrome phenotypes. Cell Rep. *12*, 1887–1901.

Ullian, E.M., Saperstein SK, Christopherson, K.S., Christopherson, K.S., and Barres, B.A. (2001). Control of synapse number by glia. Science *291*, 657–661.

Volkner, M., Zschatzsch, M., Rostovskaya, M., Overall, R.W., Busskamp, V., Anastassiadis, K., and Karl, M.O. (2016). Retinal organoids from pluripotent stem cells efficiently recapitulate retinogenesis. Stem Cell Rep. *6*, 525–538.

Weible, M.W., 2nd, and Chan-Ling, T. (2007). Phenotypic characterization of neural stem cells from human fetal spinal cord: synergistic effect of LIF and BMP4 to generate astrocytes. Glia *55*, 1156–1168.

Williams, E.C., Zhong, X., Mohamed, A., Li, R., Liu, Y., Dong, Q., Ananiev, G.E., Mok, J.C., Lin, B.R., Lu, J., et al. (2014). Mutant astrocytes differentiated from Rett syndrome patients-specific iPSCs have adverse effects on wild-type neurons. Hum. Mol. Genet. *23*, 2968–2980.

Xie, Y., Zhang, J., Lin, Y., Gaeta, X., Meng, X., Wisidagama, D.R., Cinkornpumin, J., Koehler, C.M., Malone, C.S., Teitell, M.A., et al. (2014). Defining the role of oxygen tension in human neural progenitor fate. Stem Cell Rep. *3*, 743–757.

Yan, Q., Bartz, S., Mao, M., Li, L., and Kaelin, W.G., Jr. (2007). The hypoxia-inducible factor 2alpha N-terminal and C-terminal transactivation domains cooperate to promote renal tumorigenesis in vivo. Mol. Cell Biol. *27*, 2092–2102.

Yu, J., Vodyanik, M.A., Smug-Otto, K., Antosiewicz-Bourget, J., Frane, J.L., Tian, S., Nie, J., Jonsdottir, G.A., Ruotti, V., Stewart, R., et al. (2007). Induced pluripotent stem cell lines derived from human somatic cells. Science *318*, 1917–1920.

Zhang, Y., Sloan, S.A., Clarke, L.E., Caneda, C., Plaza, C.A., Blumenthal, P.D., Vogel, H., Steinberg, G.K., Edwards, M.S., Li, G., et al. (2016). Purification and characterization of progenitor and mature human astrocytes reveals transcriptional and functional differences with mouse. Neuron *89*, 37–53.

Stem Cell Reports, Volume *8*

Supplemental Information

Hypoxia Epigenetically Confers Astrocytic Differentiation Potential on Human Pluripotent Cell-Derived Neural Precursor Cells

Tetsuro Yasui, Naohiro Uezono, Hideyuki Nakashima, Hirofumi Noguchi, Taito Matsuda, Tomoko Noda-Andoh, Hideyuki Okano, and Kinichi Nakashima

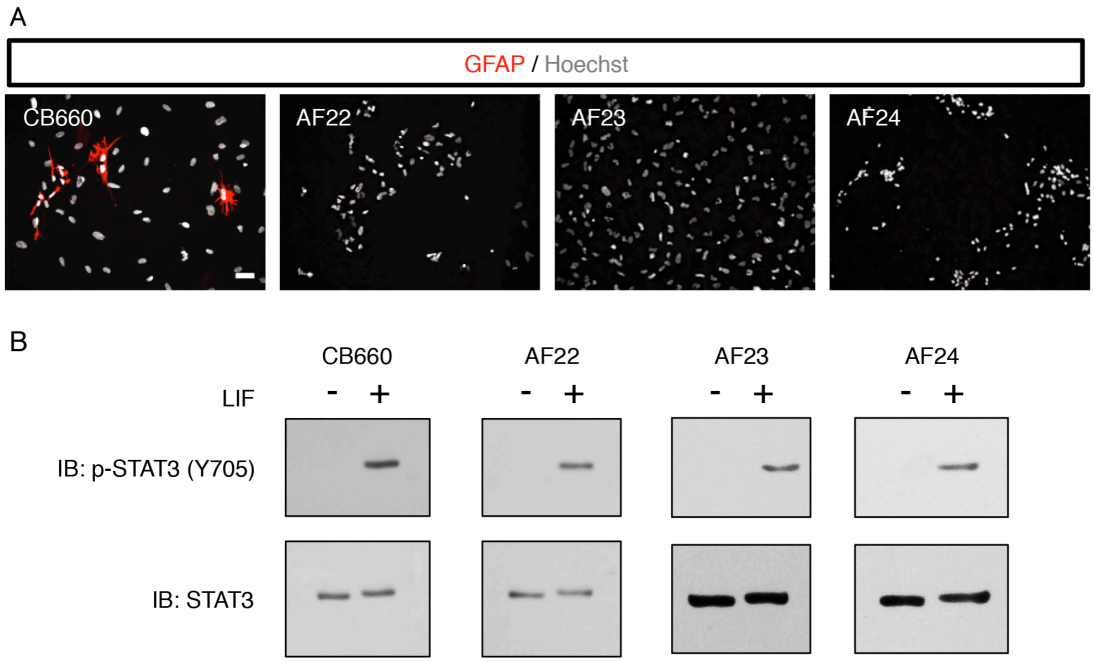

Figure S1. hNPCs derived from hPSCs fail to generate astrocytes even in the presence of LIF. Related to Figure 1.

(A) Representative images of staining for GFAP (red) and Hoechst (gray) 7 days after differentiation of hNPCs in the presence of LIF. CB660 but not AF22, 23, or 24 showed differentiation into GFAP-positive astrocytes. Scale bar = 50 μm.

(B) Western blot analysis for total and phosphorylated STAT3 in the indicated cells to assess STAT3 activation. STAT3 activation induced by LIF was observed in all cell types.

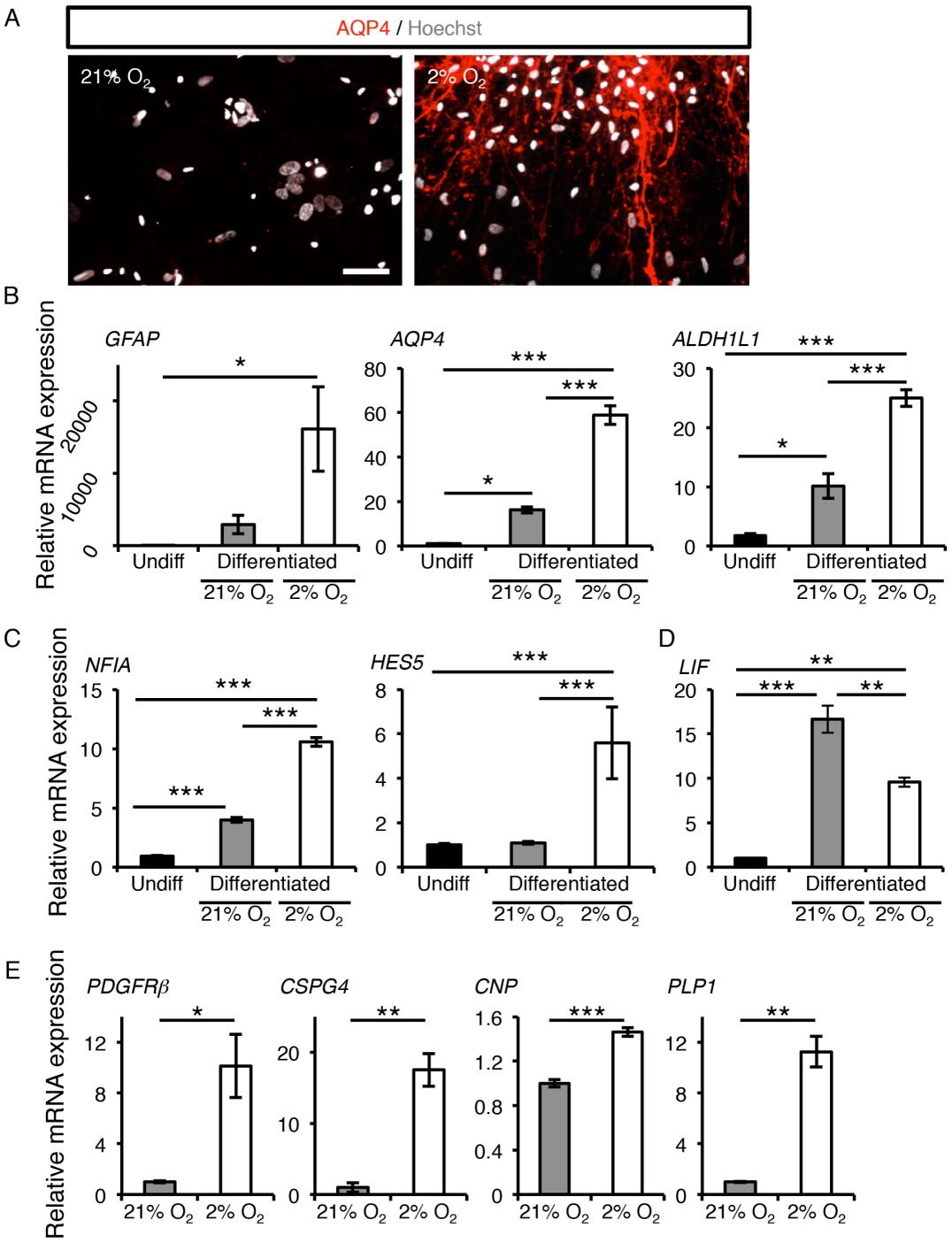

Figure S2. Glial protein and gene expressions in hPSC-derived hNPCs under hypoxia. Related to Figure 2.

(A) Immunostaining for an astrocytic marker, Aquaporin 4 (AQP4, red) after 28 days of differentiation of AF22 under normoxic or hypoxic conditions. Nuclei were counterstained with Hoechst (gray). Scale bar = 50 μm.

(B, C, D) mRNA expression levels for the indicated genes in AF22 in the undifferentiated condition

(Undiff) and 28 days of differentiation under normoxic or hypoxic conditions (n = 3 independent experiments; one-way ANOVA and Tukey's test).

(E) mRNA expression levels for the indicated oligodendrocytes-related genes in AF22 after 28 days of differentiation under normoxic or hypoxic conditions (n = 3 independent experiments; error bars are mean ± SD; $^{\star}P < 0.05$, $^{\star\star}P < 0.01$, $^{\star\star\star}P < 0.001$; Student's *t* test).

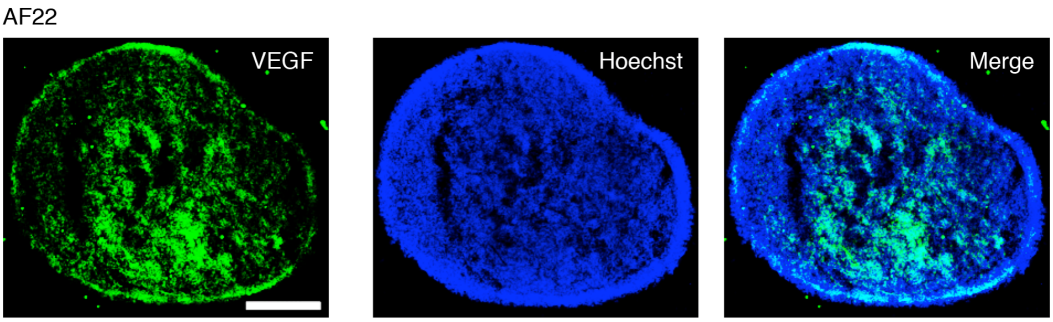

Figure S3. The HIF1α target VEGF is expressed in the hypoxic interior of hNPC aggregations. Related to Figure 3.

Representative images of staining for VEGF (green) and Hoechst (blue) of AF22 in aggregation culture under normoxia (21% O_2). Scale bar = 300 μm.

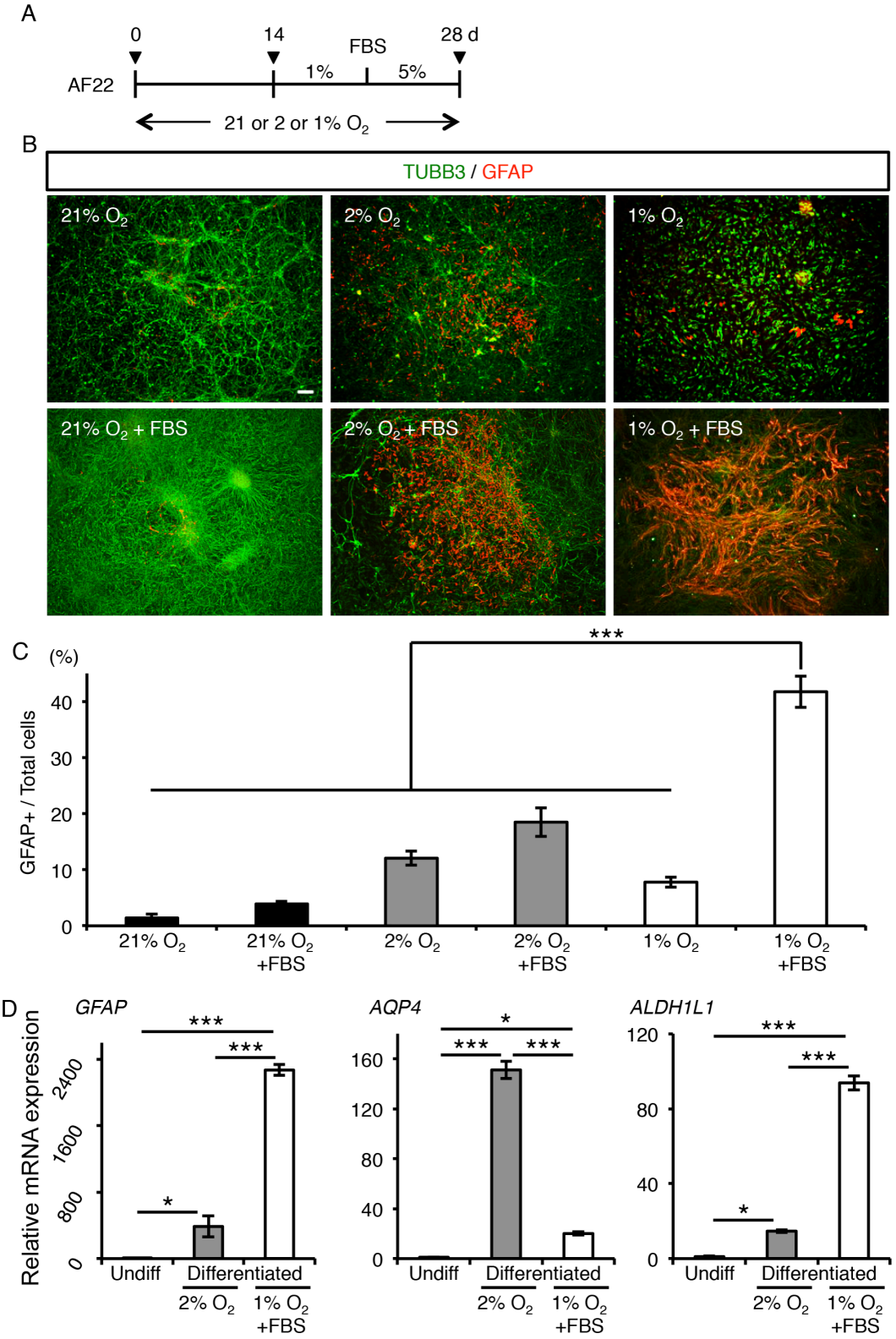

Figure S4. Astrocytic differentiation of hNPCs established from hiPSCs is further increased in the presence of FBS under 1% O_2. Related to Figure 5.

(A) Schematic representation of the modified version of the hypoxic culture. hNPCs established from hiPSCs (AF22) were cultured in differentiation medium under each oxygen concentration (21%, 2%, or 1% O_2) for 14 days without FBS, and then in the presence of FBS for 14 days.

(B) Representative images of staining for TUBB3 (green) and GFAP (red) after 28 days of differentiation of AF22 in the indicated conditions. Scale bar = 200 μm.

(C) Quantification of GFAP-positive cells in (B) for assessing differentiated statuses (n = 3 independent experiments; one-way ANOVA with Dunnett's post-test).

(D) mRNA expression levels for the indicated genes in AF22 in the undifferentiated condition (Undiff) and after 28 days of differentiation under 2% O_2 or 1% O_2 with FBS (n = 3 independent experiments; error bars are mean ± SD; $^{\star}P < 0.05$, $^{\star\star\star}P < 0.001$; one-way ANOVA and Tukey's test).

Table S1. List of primary antibodies for immunocytochemistry and western blot, related to all figures.

Antigen	Supplier	Code	Dilution	Species
Immunocytochemistry				
TUBB3	Covance	PRB-435P	1:500	rabbit
GFAP	Millipore	AB5541	1:500	chicken
GFAP	Sigma	G3983	1:500	mouse
GFP	Nacalai Tesque	GF090R	1:500	rat
DLG4	Abcam	ab2723	1:500	mouse
SLC17A7	Millipore	AB5905	1:500	guinea pig
MAP2	Millipore	AB5622	1:500	rabbit
AQP4	Santa Cruz	sc-20812	1:500	rabbit
VEGF	R&D	MAB293	1:500	mouse
Immunoblotting				
pSTAT3	Santa Cruz	sc-8059	1:1000	mouse
STAT3 (U-20)	Santa Cruz	sc-482	1:1000	rabbit
HIF1α	Novus Biologicals	NB100-479	1:500	rabbit
HIF2α	Novus Biologicals	NB100-122	1:500	rabbit
GAPDH	Millipore	MAB374	1:1000	mouse

Table S2. List of primers used in this study for qRT-PCR, related to Figure 2 and S2.

Gene	Forward primer (5'-3')	Reverse primer (5'-3')
HIF1α	TATGAGCCAGAAGAACTTTTAGGC	CACCTCTTTTGGCAAGCATCCTG
HIF1β	CTGTCATCCTGAAGACCAGCAG	CTGGTTCTCATCCAGAGCCATTC
GFAP	TGTGAGGCAGAAGCTCCAGGATGA	AGGGTGGCTTCATCTGCTTCCTGT
AQP4	GCCATCATTGGAGCAGGAATCC	ACTCAACCAGGAGACCATGACC
ALDH1L1	GGATGCCTTTGAGAATGGACGG	TCCTGGTGCTGCTCCATGAGAT
NFIA	GTGGAGGATGAAATGGACAGTCC	CTGCTGAAACCAGACTTCTCCG
HES5	TCCTGGAGATGGCTGTCAGCTA	CGTGGAGCGTCAGGAACTGCA
LIF	AGATCAGGAGCCAACTGGCACA	GCCACATAGCTTGTCCAGGTTG
PDGFRβ	TGCAGACATCGAGTCCTCCAAC	GCTTAGCACTGGAGACTCGTTG
CSPG4	GTCCTGCCTGTCAATGACCAAC	CGATGGTGTAGACCAGATCCTC
CNP	CGTGCTGCATTGCACAACCAAG	CTTGGGTGTCACAAAGAGGGCA
PLP1	GCAAGACCTCTGCCAGTATAGG	GGACAGAAGGTTGGAGCCACAA

Supplementary Experimental Procedures

Immunocytochemistry

Cells were fixed with 4% paraformaldehyde and processed for immunostaining as described (Fujimoto et al., 2012). Primary antibodies are described in Supplementary Experimental Procedures. Nuclei were stained using bisbenzimide H33258 fluorochrome trihydrochloride (Hoechst; Nacalai Tesque). All experiments were independently replicated at least three times. A Hypoxyprobe-1 Plus kit (Millipore) was used following the manufacturer's protocol to determine the hypoxicity of cultured cells. After culturing NPCs for 4 or 15 days in 2%, 21%, or 30% O_2, Hypoxyprobe-1 (pimonidazole) was added to the culture medium for 1.5 h and the cells were then fixed. Pimonidazole adducts were detected with a fluorescein isothiocyanate–conjugated specific antibody supplied with the kit (1:500). Stained sections were visualized with a fluorescence microscope (Keyence BZ9000).

Immunoblotting

Cells were lysed with a buffer containing 0.5% Nonidet P-40, 10 mM Tris-HCl, pH 7.5, 150 mM NaCl and 1% protease inhibitor mixture (Nacalai Tesque). Lysates were sonicated and centrifuged at 20,000 g for 15 min at 4°C. Total cell lysates were subjected to SDS-PAGE and transferred to a PVDF transfer membrane (GE Healthcare). The blots were blocked with 0.3% skim milk in TBST (50 mM Tris-HCl, pH 7.5, 150 mM NaCl, 0.1% Tween 20), and after incubation with a primary antibody they were washed with TBST and incubated with a peroxidase-conjugated secondary antibody. Immunoreactive bands were detected by enhanced chemiluminescence using ECL Prime Western Blotting Detection Reagent (GE Healthcare). Primary antibodies are described in Supplementary Experimental Procedures.

Morphological analysis of cultured hippocampal neurons

For analysis of neurite outgrowth, human neurons derived from AF22 were subjected to immunocytochemistry using anti-TUBB3 and anti-GFP antibodies. TUBB3-positive neurite length was measured using ImageJ software. For quantification of neuronal soma size, images were taken with a fluorescence microscope (Keyence BZ9000), and examined using ImageJ software after manual delineation of the soma margins.

Excitatory synaptic density was analyzed as previously described (Tsujimura et al., 2015). Briefly, hippocampal neurons were subjected to immunocytochemistry using anti-DLG4, anti-SLC17A7, and anti-MAP2 antibodies. DLG4 and SLC17A7 were adjudged to colocalize if markers directly overlapped or were closely apposed to each other.

Gene expression analysis

Total RNA was isolated from cells using Sepasol-RNA I Super G (Nacalai Tesque) following the manufacturer's instructions. RNA quality of all samples was checked by spectrophotometer. Reverse transcription reactions were carried out using a SuperScript VILO cDNA Synthesis Kit (Life Technologies) according to the kit protocol. qRT–PCR was performed with SYBR green fluorescent dye using Step One Plus (Applied Biosytems) and Mx3000 (Stratagene).

Supplemental Reference

Fujimoto, Y., Abematsu, M., Falk, A., Tsujimura, K., Sanosaka, T., Juliandi, B., Semi, K., Namihira, M., Komiya, S., Smith, A., et al. (2012). Treatment of a mouse model of spinal cord injury by transplantation of human induced pluripotent stem cell-derived long-term self-renewing neuroepithelial-like stem cells. Stem Cells 30, 1163-1173.